

BEAM DYNAMICS OF THE ESS SUPERCONDUCTING LINAC

M. Eshraqi, H. Danared, R. Miyamoto,
European Spallation Source, Lund, Sweden

Abstract

The European Spallation Source, ESS, uses a linear accelerator to deliver the high intensity proton beam to the target station. The nominal beam power is 5 MW at an energy of 2.5 GeV. The superconducting part covers more than 95% of the energy gain and 90% of the length. The beam dynamics criteria applied to the design of the superconducting part of the linac including the frequency jump at a medium energy of 200 MeV as well as the beam dynamics performance of this structure are described in this paper.

INTRODUCTION

The European Spallation Source, ESS, to be built in Lund, Sweden, will require a high current proton linac to accelerate protons to be used for the spallation process on which high flux of pulsed neutrons will be generated. The accelerator is a 5 MW superconducting proton linac delivering beams of 2.5 GeV to the target in pulses of 2.86 ms long with a repetition rate of 14 Hz [1], [2] corresponding to a duty cycle of 4%. Beam current is 50 mA, which at 352.21 MHz is equivalent to $\sim 9 \times 10^8$ protons per bunch. From ~ 200 MeV onward the acceleration is done at the second harmonic of the front end, 704.42 MHz, to improve the energy efficiency of the linac.

Hands on maintenance and machine protection set strict limits, 1 W/m and 0.1 W/m respectively, on beam losses and have been a concern in every high power linac [3]–[6], therefore it is crucial, specially for high power accelerators, to design a linac which does not excite particles to beam halo and also keeps the emittance growth to a minimum to avoid losing the particles that otherwise get too close to the acceptance and eventually escape the separatrix. The ESS linac is designed carefully to minimize such effects all along the linac and transfer lines. A recent study relaxed the losses in the low energy part of the linac, mainly in the RFQ and MEBT [7], from the conventional 1 W/m.

The latest design of the linac will be presented here and the 2003 Design Update can be found in Table 1 and reference [1]. In the new design it is foreseen not to exclude the possibility of a potential power upgrade of the linac. One of the scenarios for such a power upgrade would be increasing the power by increasing the energy to 3.5 GeV and/or increasing the current to 100 mA [8].

The beam dynamics of the superconducting linac as well as the handling of the frequency jump will be presented in this paper.

SUPERCONDUCTING LINAC

The superconducting linac accelerates the beam from 77.5 MeV to 201 MeV using double spoke cavities ($\beta_{opt} = 0.5$) at 352.21 MHz. The phase law in spoke section is adjusted to improve the smoothness and continuity of the phase advance between spokes and medium β cavities. This improved smoothness is achieved by ramping the synchronous phase from -20° down to -33° in the last seven periods of the spoke section. The additional effect of this change is improved acceleration in the downstream structure as well as decreasing the range of required power to accelerate the beam in medium β cavities.

The five cell elliptical cavities work at twice the frequency and increase the beam energy to 623 MeV using medium β cavities ($\beta_g = 0.67$) and then to 2.5 GeV using high β cavities ($\beta_g = 0.92$). By increasing the final energy of the spoke section and reducing the geometric β of the medium β cavities excitation of the Same Order Modes, especially $4\pi/5$, is significantly reduced at the low energy end of medium β cavities [9].

The cryomodules of the spoke and elliptical sections house two and four cavities each respectively. The transverse focusing is achieved by normal conducting quadrupole doublets. By adding a diagnostic box in between the quadrupoles as well as vacuum ports a Linac Warm Unit is formed. Each lattice period is composed of a LWU and one cryomodule in the spoke and medium β sections, or one LWU and two cryomodules in the high β section.

FREQUENCY JUMP

To allow for larger longitudinal acceptance at low energies and also ease of machining of the components a lower frequency is used at the front end of the ion accelerators. At intermediate energies is beneficial to increase the frequency to one of the higher harmonics of the bunch frequency to

Table 1: ESS Main Parameters

Parameter	Unit	2003 (LP/SP)*	2012
Ion	–	Proton / H ⁻	Proton
Energy	[GeV]	1.334	2.5
Beam power	[MW]	5.1	5
Repetition rate	[Hz]	$16\frac{2}{3} / 50$	14
Beam current	[mA]	114	50
Beam pulse	[ms]	2 / 0.48	2.86
Duty cycle	[%]	3.3 / 4.8	4

* Long pulse / Short pulse.

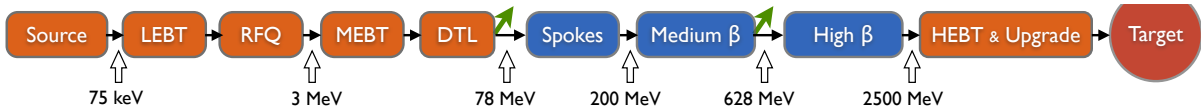


Figure 1: Block layout of the ESS segmented linac 2012 (not to scale). Orange boxes represent the normal conducting components, the blue boxes the superconducting sections, and the green arrows the branching sections.

benefit from a higher accelerating gradient and also to minimize the size of the cavities in this area. For example in the case of ESS there are around ~ 180 cavities that are run at this doubled frequency. This not only reduces their cost, but also minimizes the amount of liquid helium required for their cooling and other costs related to the transverse size of the cavities, cryo-modules and tunnel cross section.

However, such a change in the frequency causes an abrupt change in the average focusing forces in the longitudinal plane at the frequency jump according to Eq. 1, if not handled correctly, which subsequently causes a redistribution of charged particles inside the bunch, emittance dilution and enhanced halo generation.

$$k_{0l}^2 = \frac{2\pi qT \sin \phi_s}{mc^2 \beta_s^3 \gamma_s^3 \lambda} = \frac{2f_{rf} \pi qT \sin \phi_s}{mc^3 \beta_s^3 \gamma_s^3} \quad (1)$$

There has been studies [10, 11] proposing solutions to avoid this unwanted effects. One of the drawbacks of these methods is that they find solutions by only adjusting the structure which comes downstream of the frequency jump. Figure 2 shows the phase advance per unit length, square root of the average focusing force, and average energy gain per meter, and power consumption per cavity when the frequency jump is handled using the method discussed in reference [11].

The frequency change in the earlier ESS linac, 2011 Baseline [12], happens at around 50 m in Fig. 2. To keep the same longitudinal acceptance the synchronous phase is decrease to twice its value before the frequency jump, Fig. 3. To smoothen the variation of the average phase advance across the frequency jump the accelerating gradient in the medium beta section, the first section downstream of the frequency jump, is reduced. This causes an energy gain per meter of ~ 0.5 MeV/m, and the power per cavity is reduced to less than ~ 50 kW. The latter requires a specific coupler design for these cavities and also reduces the efficiency of the power sources for these cavities significantly.

These two are mainly caused since the average phase advance should be matched to that of the upstream structure. One could equally well increase the average phase advance in the upstream structure by lowering the synchronous phase gradually in the upstream structure, e. g. the spoke section in the ESS linac. The 2012 ESS linac uses this new scheme to enhance the acceleration in the overall linac. On Fig. 4 and 5, at ~ 40 m, the average phase advance is almost equal to the target average phase advance in the medium beta section. From this point on the synchronous phase gradually decreases towards -35° to keep the average phase advance constant. This diminishes the

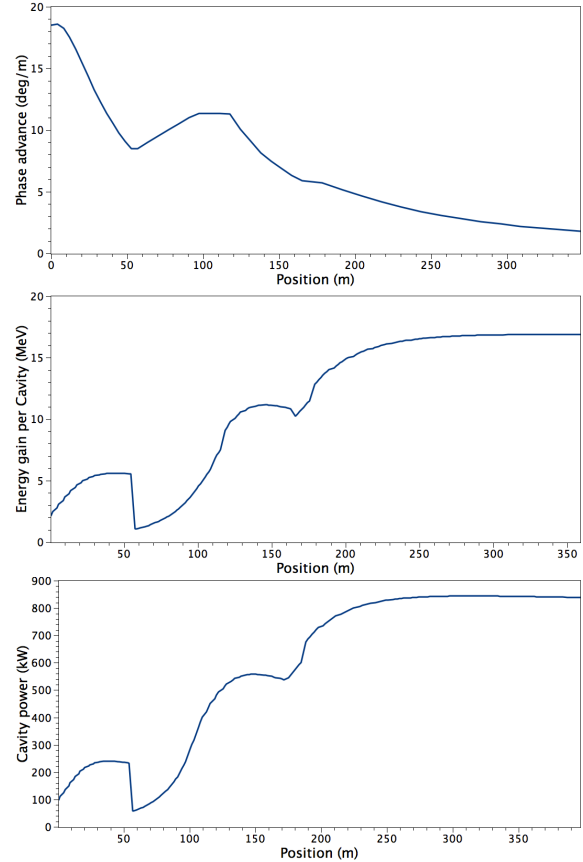


Figure 2: Top: phase advance per unit length, middle: average energy gain per meter, bottom: power consumption per cavity in the ESS 2011 SC linac.

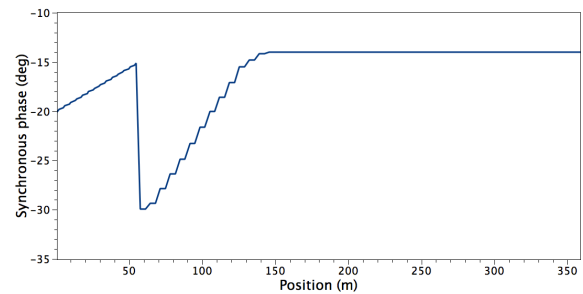


Figure 3: Synchronous phase in the ESS 2011 SC linac.

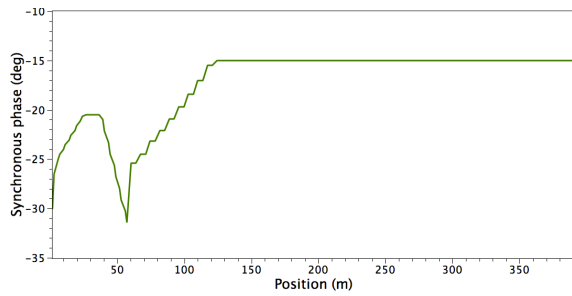


Figure 4: Synchronous phase in the ESS 2012 SC linac.

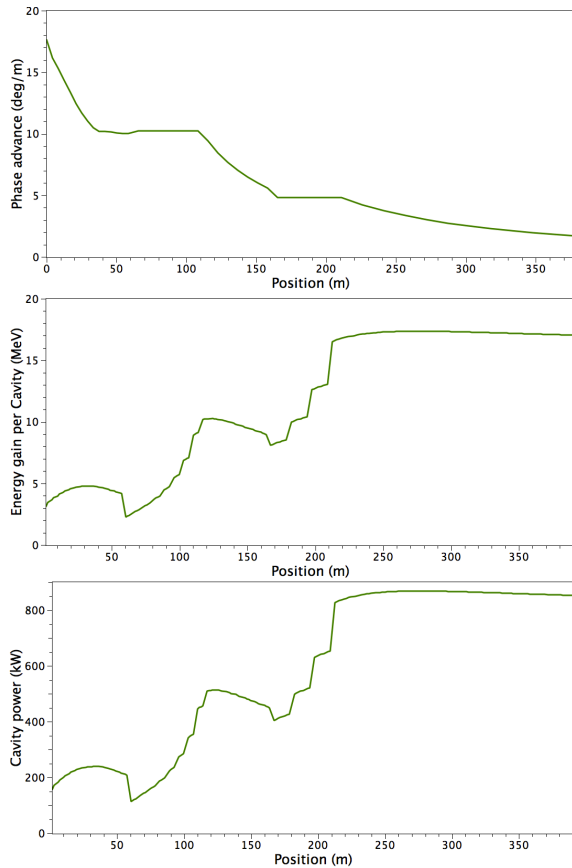
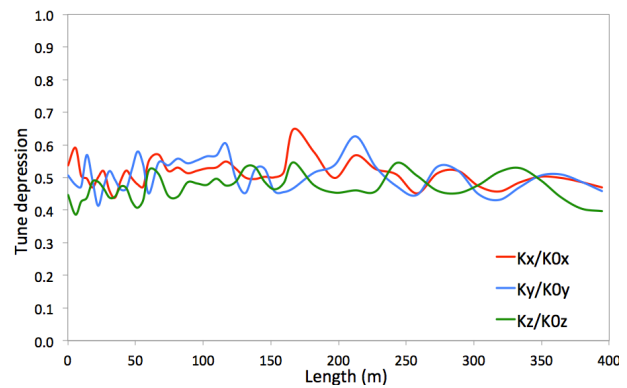


Figure 5: Top: phase advance per unit length, middle: average energy gain per meter, bottom: power consumption per cavity in the ESS 2012 SC linac.

acceleration efficiency in the spoke section to $\sim 96\%$ of its original value where the synchronous phase was -14° , but since the accelerating gradient in the medium beta section is higher this minor loss of energy gain could easily be recovered in few cavities of the medium beta section.

In the 2012 ESS SC linac the average energy gain per cavity in the medium beta section is increased to ~ 2.3 MeV/m, which is more than twice the energy gain in the 2011 ESS baseline. At the same time the power per cavity is increased from ~ 50 kW to ~ 130 kW, reducing the range of the power per cavity from ~ 13 to ~ 4 .

The real estate gradient over the active length is in-

Figure 6: Tune depression evolution vs. length. *Length measured from the beginning of SC linac.*

creased from 13.388 MeV/m in the 2011 ESS SC linac to 13.731 MeV/m in the 2012 ESS SC linac. Though the difference is not significant, this change results in an extra ~ 137 MeV of energy over ~ 400 m length of the ESS SC linac. Since the linac layout has changed significantly from the 2011 baseline to 2012 baseline, the real estate gradients were calculated only over the total length of the cavities, excluding the effect of different filling factors in the two linacs that has decreased from 0.505 in 2011 to 0.454 in 2012.

BEAM DYNAMICS

The new design of the linac is focused on improving the integrity of the accelerator as a single structure and improving the real estate gradient while the progress in the mechanical drawing of components has been reducing the filling factor. The guidelines on the design of the linac are:

- The transverse phase advance per period is limited to 87° to reduce the percentage of the beam that due to their phase otherwise would have had a phase advance exceeding 90° per period.
- The smooth and monotonic variation of the average phase advance.
- At the same time the tune depression is being kept above 0.4 limiting the number of mismatch resonances to only two, Fig. 6, from which one is always present irrespective of the tune depression and to avoid the second resonance one should keep the tune depression above ~ 0.6 , Fig. 7 [13].
- Since the tune depression is very close to 0.4, unless the beam is equipartitioned tune depression will be less than 0.4 at least in one plane. This limits the longitudinal phase advance per period to 73° , permitting to keep the linac almost equipartitioned in large part of the linac.

Though every section of the accelerator is designed to match the average phase advance of neighboring structures,

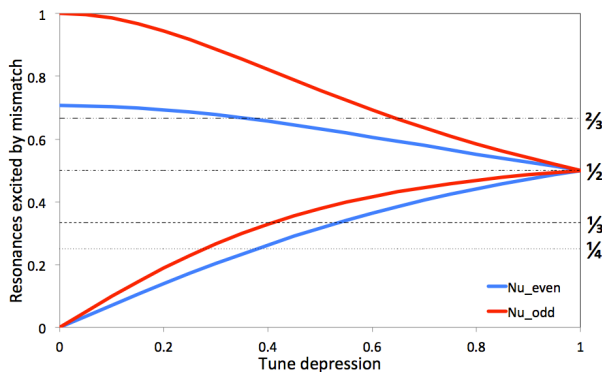


Figure 7: Mismatch excited resonances vs. tune depression.

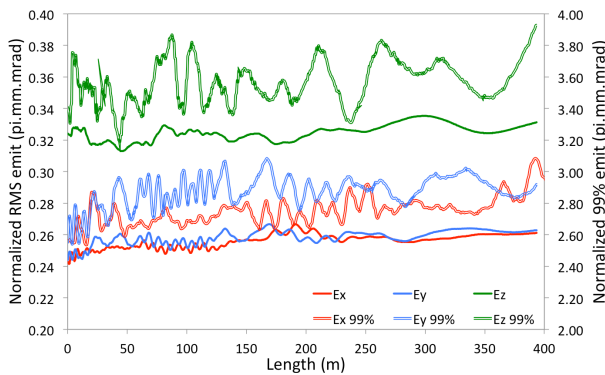


Figure 8: RMS and 99% emittance evolution vs. length. Length measured from the beginning of SC linac.

a further phase advance smoothness matching is performed during the integration to assure a premium beam quality.

The Start2End (End2End) simulations are performed with 100,000 macro particles using the code TRACEWIN [14]. The 3D PICNIC space charge routine with a $10 \times 10 \times 10$ mesh is employed for space charge calculations, which are performed 25 times per $\beta \cdot \lambda$, a limit that speeds up the calculation and does not affect the results. This beam is generated at the RFQ input and transported through the linac and HEBT to the target wheel surface. However, this paper covers only the SC linac.

The aperture to rms beam size in the SC linac stays above 10 and 8 in transverse and longitudinal planes respectively. The emittance growth from the input to the SC linac, end of the DTL, to the end of linac are 8%, 7% and 2% in xx' , yy' , and zz' planes, Fig. 8. The simulations use a beam which has already been tracked through the normal conducting front end.

The sensitivity of linac to the Same Order Modes and Higher Order Modes have been studied [9] confirming that none of these modes are excited, especially at the extremities of each of the three accelerating structures.

ERROR STUDIES

To define the tolerances on the active elements, a set of statistical runs applying errors on the alignment and field vectors of quadrupoles and cavities have been performed. These studies are broken in two steps, firstly to define the tolerances on each variable, e.g. only quadrupole alignment, and its effect, and secondly applying all the errors, weighted to have comparable effects, to simulate the effect. The study was performed using 100,000 macro particles, with the same space charge routine and settings as for the beam dynamics studies, over 1000 linacs, on each of them the variable under study is varied uniformly between zero and *maximum error* \times *step of error*.

The quadrupole errors are applied in three different set of runs:

- Alignment, i.e. ΔX and ΔY , up to 0.5 mm, divided in five steps. The effect of rotation around x and y axes, pitch and yaw, was found to be negligible.
- Roll angle, i.e. rotation around the z -axis $\Delta\phi_z$, up to 0.25° corresponding to 4 mrad in five steps.
- Gradient errors, ΔG , up to 2% divided in four steps.
- The effect of higher order components of the magnetic field is still under study.

The cavity errors are applied in three sets of runs

- Alignment error of the cavity ΔX . Up to 5 mm in five steps. Due to symmetry it was assumed that for the ΔY the same value could be tolerated.
- Cavity pitch, rotation around the x axis, $\Delta\phi_x$, up to 5 mrad in five steps. Due to symmetry rotation around the y axis is not studied.
- Accelerating field errors, ΔE_{acc} , up to 2.5% divided in five steps.
- The phase of the accelerating field, $\Delta\phi_s$, up to 2.5° divided in five steps.
- Due to cylindrical field symmetry the errors in roll of the cavities, rotation around the z axis is not studied.

After this first set of studies the new boundaries are found and distributed almost fairly amongst the different variables. The applied errors for the second set of studies is limited to $\Delta X_Q, Y_Q < 0.3$ mm, $\Delta\phi_{zQ} < 1$ mrad, and $\Delta G < 0.75\%$ for the quadrupoles, and to $\Delta X_C, Y_C < 3$ mm, $\Delta\phi_x, \phi_y < 3$ mrad, $\Delta\phi_s < 1.5^\circ$, and $\Delta E_{acc} < 1.5\%$ for the cavities, all parameters varied together in three steps. There has not been any particles lost in these simulations, the results are reported in Table 2.

The maximum beam radius for the three steps of the error is plotted in Fig. 9. Considering the fact that the input beam jitter has not been included in these studies, one should be careful not to consume all the available margin

Table 2: Results of the Error Study Reported as $Average \pm \sigma$

Parameter	1/3	2/3	3/3
$\Delta\epsilon_x^*[\%]$	6.50 ± 3.37	23.31 ± 9.71	47.02 ± 21.99
$\Delta\epsilon_y[\%]$	7.33 ± 3.61	25.80 ± 11.33	50.51 ± 23.69
$\Delta\epsilon_z[\%]$	17.47 ± 7.73	56.77 ± 17.50	94.47 ± 34.66
Halo _x	1.97 ± 0.12	1.91 ± 0.32	1.94 ± 0.42
Halo _y	1.96 ± 0.13	1.88 ± 0.34	1.91 ± 0.45
Halo _z	2.06 ± 0.26	1.67 ± 0.41	1.46 ± 0.53
$x'_\sigma [\text{mrad}]$	0.078	0.149	0.235
$y'_\sigma [\text{mrad}]$	0.082	0.173	0.250
$\alpha_{xy\sigma}$	0.024	0.058	0.081
$\alpha_{x'y'_\sigma}$	0.012	0.028	0.045

* The $\Delta\epsilon_s$ are the additional emittance growth wrt to the nominal output.

‡ For angles and α_s just the σ is reported.

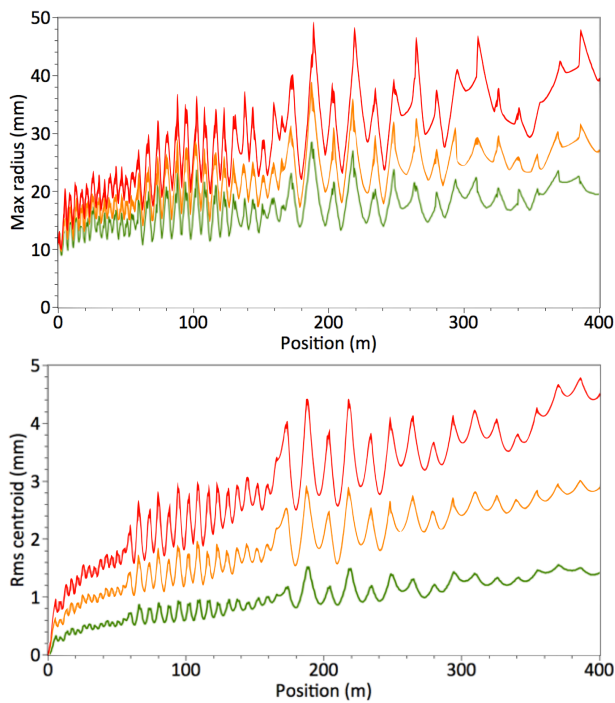


Figure 9: Top: maximum beam radius in case of errors, bottom: rms beam centroid, green 1/3, amber 2/3, red 3/3 of the maximum error applied.

without taking into account the effect of upstream structures on the beam. Therefore one can argue that the limit should be 2/3 of the errors defined in previous paragraph. Though yet the beam center has not been corrected, but the beam size in the high beta region is specially dominated by the envelope oscillations and not by the beam center random walk, Fig. 9.

SUMMARY

The beam dynamics of the SC linac of the ESS was presented with emphasis on the new method to handle the fre-

quency jump in this linac. The sensitivity of the linac to a set of defined errors was checked and the results of the error study were presented. The linac is designed respecting the rules of the thumb in high intensity ion linacs, namely smooth and monotonic variation of phase advance, 87° upper limit on phase advance and avoiding resonances have resulted in a robust design. Simulations show that the beam quality is preserved in the nominal case and even when realistic errors or the SOM and HOM are applied the linac transports and accelerates the beam without affecting the beam quality or inducing any losses.

ACKNOWLEDGMENTS

We would like to thank Romuald Duperrier and the ADU collaboration for their input and suggestions.

REFERENCES

- [1] “ESS Volume III Update: Technical report status”, 2003, <http://ess-scandinavia.eu/documents/VolIII.pdf>
- [2] S. Peggs, Ed., “The conceptual design report”, 2011, <http://ess-scandinavia.eu/ess-documents/589-cdr>
- [3] R. A. Jameson, “Design for low beam loss in accelerators for intense neutron source applications”, PAC1993.
- [4] T. P. Wangler, E. R. Gray, F. L. Krawczyk, S. S. Kurennoy, G. P. Lawrence, R. D. Ryne and K. R. Crandall, “Basis for low beam loss in the high-current APT linac”, LINAC98.
- [5] J. L. Biarrotte, A. C. Mueller, H. Klein, P. Pierini and D. Vandeplasseche, “Accelerator reference design for the MYRRHA European ADS demonstrator”, LINAC10.
- [6] D. Raparia, J. Alessi, B. Briscoe, J. Fite, O. Gould, V. Lo Destro, M. Okamura, J. Ritter and A. Zelenski, “Reducing losses and emittance in high intensity linac at BNL”, HB2010.
- [7] L. Tchelidze, J. Stovall, “Estimation of residual dose rates and beam loss limits in the ESS linac”, ESS AD Technical Note, ESS/AD/0039.
- [8] M. Lindroos, H. Danared, M. Eshraqi, D. P. McGinnis, S. Molloy, S. Peggs, K. Rathsmann, R. D. Duperrier and J. Galambos, “Upgrade strategies for high power proton linacs”, IPAC10.
- [9] Rob Ainsworth, *private communication*.
- [10] R. Duperrier, N. Pichoff, D. Uriot, “Impact of a RF frequency change on the longitudinal beam dynamics”, Proceedings of LINAC 2006, Knoxville, Tennessee USA.
- [11] R. Duperrier, N. Pichoff, and D. Uriot, Phys. Rev. ST Accel. Beams, **10**, 084201, (2007).
- [12] M. Eshraqi, H. Danared, “ESS LINAC, Design and Beam Dynamics”, Proceedings of IPAC11, San Sebastian, Spain.
- [13] J. M. Lagniel, “Halos and chaos in space-charge dominated beams”, EPAC96.
- [14] R. Duperrier, N. Pichoff and D. Uriot, Proc. International Conf. on Computational Science, Amsterdam, The Netherlands, 2002.